SHORT REPORT

Developmental Science   WILEY

Revisiting brain rewiring and plasticity in children born without corpus callosum

Vanessa Siffredi[1,2,3,4] | **Maria G. Preti**[1,2,5] | **Silvia Obertino**[1,2] | **Richard J. Leventer**[6,7,8] | **Amanda G. Wood**[3,9,10] | **Alissandra McIlroy**[3] | **Vicki Anderson**[3,8,11,12] | **Megan M. Spencer-Smith**[3,13] | **Dimitri Van De Ville**[1,2,5]

[1] Medical Image Processing Lab, Institute of Bioengineering, Center for Neuroprosthetics, Ecole Polytechnique Fédérale de Lausanne, Lausanne, VD, Switzerland

[2] Department of Radiology and Medical Informatics, Faculty of Medicine, University of Geneva, Geneva, Geneva, Switzerland

[3] Brain and Mind Research, Clinical Sciences, Murdoch Children's Research Institute, Melbourne, Australia

[4] Division of Development and Growth, Department of Paediatrics, Faculty of Medicine, University of Geneva, Geneva, Geneva, Switzerland

[5] CIBM Center for Biomedical Imaging, Switzerland

[6] Department of Paediatrics, University of Melbourne, Melbourne, Australia

[7] Department of Neurology, Royal Children's Hospital, Melbourne, Australia

[8] Neuroscience Research, Clinical Sciences, Murdoch Children's Research Institute, Melbourne, Australia

[9] School of Life and Health Sciences & Aston Neuroscience Institute, Aston University, Birmingham, UK

[10] School of Psychology, Faculty of Health, Melbourne Burwood Campus, Deakin University, Geelong, Victoria, Australia

[11] School of Psychological Sciences, University of Melbourne, Melbourne, Australia

[12] Department of Psychology, Royal Children's Hospital, Melbourne, Australia

[13] Turner Institute for Brain and Mental Health, School of Psychological Sciences, Monash University, Melbourne, Australia

Correspondence
Vanessa Siffredi, Campus Biotech, Chemin des Mines 9, 1211 Genève, Geneva, Geneva, Switzerland.
Email: vanessa.siffredi@unige.ch

Megan M. Spencer-Smith and Dimitri Van De Ville contributed equally to this work.

Abstract

The corpus callosum is the largest white matter pathway connecting homologous structures of the two cerebral hemispheres. Remarkably, children and adults with developmental absence of the corpus callosum (callosal dysgenesis, CD) show typical interhemispheric integration, which is classically impaired in adult split-brain patients, for whom the corpus callosum is surgically severed. Tovar-Moll and colleagues (2014) proposed alternative neural pathways involved in the preservation of interhemispheric transfer. In a sample of six adults with CD, they revealed two homotopic bundles crossing the midline via the anterior and posterior commissures and connecting parietal cortices, and the microstructural properties of these aberrant bundles were associated with functional connectivity of these regions. The aberrant bundles were specific to CD and not visualised in healthy brains. We extended this study in a developmental cohort of 20 children with CD and 29 typically developing controls (TDC). The two anomalous white-matter bundles were visualised using tractography. Associations between structural properties of these bundles and their regional functional connectivity were explored. The proposed atypical bundles were observed in 30% of our CD cohort crossing via the anterior commissure, and in 30% crossing via the posterior commissure (also

observed in 6.9% of TDC). However, the structural property measures of these bundles were not associated with parietal functional connectivity, bringing into question their role and implication for interhemispheric functional connectivity in CD. It is possible that very early disruption of embryological callosal development enhances neuroplasticity and facilitates the formation of these proposed alternative neural pathways, but further evidence is needed.

1 | INTRODUCTION

The corpus callosum is a central structure within the human brain. With >250 million axons, it is the largest commissural bridge of white-matter bundles connecting the left and the right hemispheres. It plays a crucial role in transmitting sensory, motor, and higher level cognitive information between homotopic regions of the two cerebral hemispheres (Gazzaniga, 2000; Paul et al., 2007). The corpus callosum develops prenatally so that by 20 gestational weeks, it has reached its final shape, but will continue to mature postnatally with myelination finally completed during early adulthood (Edwards et al., 2014; Giedd et al., 1996; Pujol et al., 1993).

Callosal dysgenesis (CD) describes a collection of brain malformations in which the corpus callosum fails to develop prenatally either completely or partially, that is, complete CD, also called complete agenesis of the corpus callosum, and partial CD. Remarkably, individuals with CD show little evidence of the classical disconnection syndrome and do not manifest impairment in interhemispheric integration, as instead observed in split-brain patients. Moreover, functional connectivity studies in CD individuals report relatively preserved interhemispheric connectivity (Mancuso et al., 2019; Siffredi et al., 2020; Tyszka et al., 2011).

Diffusion tensor imaging and fibre tractography have been previously used to explore structural connectivity in individuals with CD. Bénézit et al. (2015) showed overall preserved organisation of the main white matter bundles in children with CD, but revealed reduced whole-brain global connectivity and increased local connectivity in individuals with complete CD compared with healthy controls using connectomics approaches examining structural connectomes (Meoded et al., 2015; Owen et al., 2013). Analysing structural connectivity data within and across hemispheres, previous work has also reported a pattern of decreased inter-hemispheric but increased intra-hemispheric structural connectivity in individuals with CD (Siffredi et al., 2020; Yuan et al., 2020). These findings are in line with the previously proposed hypothesis of structural strengthening of intra-hemispheric pathways as a neuroplastic response in the acallosal brain (Chiarello, 1980; Dennis, 1976).

Another hypothesis of neuroplastic response is the existence of alternative neural pathways crossing the midline via the anterior and posterior commissures and proposed to be involved in the preserva-

tion of interhemispheric transfer in individuals with CD. In typically developing brains, the anterior commissure contains fibres connecting temporal areas, including the temporal poles and the inferior temporal cortex, as well as occipital areas with the inferior occipital gyri (Catani & Thiebaut de Schotten, 2008; Kollias, 2012). The posterior commissure is an exclusively subcortical, mesodiencephalic bundle that makes direct connections with the nucleus of Darkschewitsch and the red nucleus, as well as with the habenular nuclei (Keene, 1938). Tovar-Moll et al. (2014) proposed that CD is associated with a brain rewiring process, showing the presence of two homotopic interhemispheric bundles crossing the midline through the anterior and the posterior commissures and connecting parietal cortices. These aberrant interhemispheric bundles, namely the ventral forebrain and midbrain bundles, previously unreported, were visualised in addition of the typical connections of the anterior and posterior commissures and were not visualised in healthy brains. Specifically, in their sample of six individuals with CD, the ventral forebrain bundle was observed in one individual with partial CD, and the midbrain bundle was observed more frequently in four individuals with CD (one complete CD, two partial CD and one with hypoplasia).

Resting-state functional connectivity MRI (rsfMRI) measures the spontaneous synchronized fluctuations in blood oxygen level-dependent (BOLD) signal during awake rest (Bolton et al., 2020; Supekar et al., 2009; Uddin et al., 2010). This method allows to evaluate the statistical interdependence between regional activity timecourses, termed functional connectivity (FC). FC measures derived from rsfMRI data have become a powerful tool to investigate functional organization of brain networks in typical and atypical development. In individuals with CD, (Tovar-Moll et al., 2014) observed an association with resting-state FC in parietal areas and the structural connectivity values of the aberrant bundles. These findings supported the hypothesis of the potential functional role of these bundles in the preservation of functional interhemispheric transfer.

The current study aimed to investigate further the presence of these alternative interhemispheric bundles and brain rewiring in a large developmental cohort. To this end, the study of Tovar-Moll and colleagues was extended by investigating the presence of the ventral forebrain and midbrain bundles in a large cohort of children with CD compared with typically developing control (TDC) children. To further explore evidence of their potential functional role in the preservation

of interhemispheric transfer, associations between the structural properties of these bundles and their regional FC was explored.

Based on the results of Tovar-Moll and colleagues we expected few children in our cohort would show the ventral forebrain bundle crossing the midline through the anterior commissure, while the majority would show the midbrain bundles crossing the midline via the posterior commissure

2 | METHODS

2.1 | Sample

This study used data from the "Paediatric Agenesis of the Corpus Callosum Project" from The Royal Children's Hospital (RCH), Melbourne, Australia (Siffredi et al., 2018). Inclusion criteria were: aged 8 to 16 years; evidence of CD on MRI; English speaking; and functional ability to engage in the assessment procedure. A cohort of 28 children with CD was recruited from clinics and radiology records at The RCH. Inclusion criteria were: (1) aged 8 years 0 months to 16 years and 11 months; (2) documented evidence of CD on Magnetic Resonance Imaging (MRI) conducted as part of a routine clinical work-up; (3) English speaking; and (4) functional ability to engage in the assessment procedure. MRI findings were qualitatively reviewed by a paediatric neurologist with expertise in brain malformations (RJL), who confirmed diagnosis of CD, including complete and partial CD, and identified associated brain malformations. A TDC group of 30 children comparable in age and sex to the CD group was recruited through advertisement in local schools and through staff at The RCH.

The project was approved by the RCH Human Ethics Research Committee. Caregivers provided written informed consent prior to participation.

2.2 | Neuroimaging

2.2.1 | Magnetic resonance imaging acquisition

Images were acquired on a 3T MAGNETOM Trio scanner (Siemens, Erlangen, Germany) at The RCH. A 32-channel head coil was used for transmission and reception of radio-frequency and signals. Before the MRI, all participants successfully completed a mock MRI training protocol. A high-resolution 3D anatomical image was acquired using a T1-weighted MP-RAGE sequence (TR = 1900 ms, TE = 2.71 ms, TI = 900 ms, FA = 9°, FoV = 256 mm, voxel size = 0.7 × 0.7 × 0.7 mm). Echo planar diffusion-weighted imaging (DWI) data were acquired at two different b-values, including two scans without diffusion weighting (b-factor = 0): (a) b-value = 3000s/mm2, 50 gradient directions where 54 slices with isotropic voxels of 2.3 × 2.3 × 2.3 mm were obtained (TR = 8200 ms; TE = 112 ms; FoV = 240 mm; axial slice orientation with phase encoding in the anterior–posterior direction) with an acquisition time of 6.8 minutes; and (b) b-value = 1000s/mm2, 30 gradient directions where 64 slices with isotropic voxels of 2 × 2 × 2 mm

RESEARCH HIGHLIGHTS

- In callosal dysgenesis, brain rewiring has been proposed via alternative white-matter bundles crossing the midline through the anterior and posterior commissures
- In a large developmental cohort, these aberrant commissural bundles were observed in less than half of the cohort
- The presence and structural properties of the aberrant bundles were not associated with functional connectivity
- Our findings bring into question the role and implication of these aberrant bundles in alternative pathways for interhemispheric functional connectivity in callosal dysgenesis

were obtained (TR = 8600 ms; TE = 90 ms; FoV = 256 mm; axial slice orientation with phase encoding in the anterior–posterior direction) with an acquisition time of 4.3 minutes. Resting-state gradient-echo EPI sequences was also acquired (196 slices, TR = 2000 ms, TE = 30 ms, voxel size: 2.6 × 2.6 × 4 mm, FA: 90 deg, FoV = 250 mm × 250 mm), with an acquisition time of 6.5 minutes. During the resting-state functional MRI (fMRI) sequence, participants were instructed to keep their eyes closed and try not to think of anything.

2.2.2 | DWI preprocessing and probabilistic tractography

Diffusion weighted imaging (DWI) scans were converted from the native DICOM to NIFTI format using the dcm2nii tool developed at the McCauseland Centre for Neuroimaging (http://www.mccauslandcenter.sc.edu/mricro/mricron/dcm2nii.html). Each image was visually checked gradient by gradient and slice by slice. One participant was excluded due to artefacts linked to head motion, and one participant was excluded due to difficulties characterising corpus callosum malformation. DWI data sets were preprocessed for tractography using MRtrix 3 (Tournier). DWI data denoising, eddy current-induced distortion correction, motion correction, and bias field correction were performed on the two different shells independently. In order to remove non-brain tissue components and background noise, b0 images for the two shells were extracted using Brain Extraction Tool (BET2) compiled in FSL (S. M. Smith, 2002). Images from the two shells were then coregistered using FreeSurfer and merged using FSL. An in-house global normalisation procedure of the two shell DWI data was performed (Obertino et al., 2017). Tractography and connectome reconstruction were done using MRtrix 3 (Tournier; Tournier et al., 2008; Tournier et al., 2007). The Tax algorithm was used for single-fibre voxel selection and response function estimation (Tax et al., 2014). The second order integration over fibre orientation distributions (iFOD2) algorithm was estimated using constrained spherical deconvolution with default parameters (Tournier et al., 2008). Probabilistic tractograms of one million streamlines were generated over the entire brain, with sub-

sequent filtering to 100 thousands streamlines using Spherical Deconvolution Informed Filtering of Tractograms (SIFT) to improve the accuracy of the reconstructed whole-brain connectome (R. E. Smith et al., 2013). The streamlines crossing the midline through the anterior and posterior commissures were tracked using a multiple ROI approach consisting of placing a bilateral ROI in parasagittal slices in the topography of the anterior or posterior commissure (Tovar-Moll et al., 2014). ROIs were manually defined by overlaying each participant's FA map with the co-registered T1-weighted image (Siffredi et al., 2019). The resulting tracts were exported to TrackVis format for visualisation and selection of the streamlines of interest, that is, the midbrain and ventral forebrain bundles (Catani & Thiebaut de Schotten, 2008). For the selection of the streamline of interest, the following guideline was used: a minimum number of one tract for a given bundle crossing through either the anterior or posterior commissures and connecting parietal cortices inter-hemispherically, the registered Brainnectome atlas was also used to confirmed that most streamlines connect parietal areas (Fan et al., 2016). Number of streamlines, tract volumes, and mean FA measures along these bundles were extracted.

2.2.3 | Resting-state functional MRI preprocessing and functional connectivity associated with alternative bundles

Resting-state functional MRI (fMRI) data were converted from the native DICOM to NIFTI format using dcm2nii. For each participant, the first five (of the 196) volumes were discarded to ensure magnetisation equilibrium, and the remainder underwent spatial realignment and smoothing (5 mm FWHM Gaussian kernel) using SPM12 (Wellcome Centre for Human Neuroimaging, University College London, UK, http://www.fil.ion.ucl.ac.uk/spm/software/spm12). For resting-state fMRI data, the mean framewise displacement for each frame was computed to quantify the extent of head motion from volume to volume for each participant (Power et al., 2014; Power et al., 2012). Following Power et al. recommendations (2012; 2014), we implemented volume censoring (i.e., scrubbing) for motion correction using a framewise displacement of 0.5 mm threshold for exclusion. Participants with less than 125 frames remaining after scrubbing were excluded. Using this approach, three CD and one TDC participants were removed from further analyses. The following steps were performed on the scrubbed data of all remaining participants. We followed the preprocessing pipeline described by Preti and Van De Ville (2017). Voxelwise timecourses were first detrended (linear and quadratic trends). The six motion parameters, as well as the average white matter and cerebrospinal fluid signals obtained from standard white matter and ventricular masks mapped to the subject's fMRI space and masked with individual segmentation maps, were regressed out using the DPARSF toolbox (Leonardi et al., 2013). The timecourses were then band-pass filtered in the range of [0.01 0.15 Hz] to enhance resting-state fluctuations. To restrict the analysis to voxels belonging to grey matter, the segmented grey matter T1 image obtained using SPM12 was resliced and coregistered to each individual's mean functional image, and used

as a mask. The Brainnetome Atlas was also resliced and coregistered to each individual's T1 image coregistered to the mean functional image. Quality check of the coregistation of the atlas to the individual's T1 image coregistered to the mean functional image were carefully done for cortical and subcortical regions. Region-averaged time series were extracted in each participant's individual space. To explore associations between structural properties of the two aberrant commissural bundles previously identified to connect interhemispherically parietal cortices and their regional functional connectivity, we used two different approaches:

a. Pairwise Pearson's correlation coefficients were computed between functional timecourses of the regions connected by the aberrant bundles, defined as atlas-based seeds. Atlas-based seeds correspond to regions of the Brainnetome Atlas (Fan et al., 2016) in which left and right sided streamlines from the two bundles end for all participants. As the ventral forebrain and the midbrain bundles connect partial areas, the atlas-based seeds were located in parietal lobes.

b. Pairwise Pearson's correlation coefficients were computed between functional timecourses of the regions connected by the aberrant bundles, defined as bundle-specific seeds. The bundle-specific seeds correspond to left and right sided endpoints for the two bundles of interest. Endpoints of the streamlines were extracted for both hemispheres and a sphere of 5 mm was considered around each endpoint for each participant. These subject specific ROIs were coregistered and resliced to the functional space, and two seeds were created (one for each hemisphere). Given that the ventral forebrain and the midbrain bundles connect partial areas, the bundle-specific seeds were located in parietal lobes.

2.3 | General intellectual functioning measure

To evaluate general intellectual functioning, the Wechsler Abbreviated Intelligence Scale (WASI: Wechsler, 1999) or the Wechsler Intelligence Scale for children—Edition IV (WISC-IV: Wechsler, 2003) was administered and a Full-Scale Intellectual Quotient (IQ) score was calculated, mean (M) = 100 and standard deviation (SD) = 15.

2.4 | Statistical analyses

To evaluate the presence of the ventral forebrain and midbrain bundles, the percentage of visualization of these bundles were reported for each group. Chi-square analyses were performed to compare proportional differences in the visualization of the ventral forebrain and midbrain bundles between the CD and the TDC groups.

To evaluate group differences on general intellectual functioning (i.e., full-scale IQ scores) between CD children for whom the aberrant commissural bundles were visualised on tractography and those for

TABLE 1 Characteristics of the callosal dysgenesis (CD) and typically developing control (TDC) groups

	CD	TDC	Group comparison
Tractography analysis			
n	20	29	–
Age in years, mean (SD)[range]	12.08 (2.63) [8.67-17.08]	11.75 (2.32) [8-16.42]	$t(47) = 0.048, p = 0.642$
Sex, n	7 females, 13 males	13 females, 16 males	$X^2(1, n = 49) = 0.473, p = 0.491$
Handedness, n	11 R, 8 L, 1 M	26 R, 3 L	$X^2(2, n = 49) = 7.970, p = 0.019$
Full-Scale IQ, median [range]	75.5 [66-126]	113 [88−136]	$W = 964.5, p < 0.001$
Association between tractography and microstructural properties with functional connectivity (FC)			
n	16	28	–
Age in years, mean (SD)[range]	12.16 (2.75) [8.67-17.08]	11.71 (2.35) [8-16.42]	$t(42) = 0.567, p = 0.572$
Sex, n	6 females, 10 males	12 females, 16 males	$X^2(1, n = 44) = 0.121, p = 0.728$
Handedness, n	10 R, 5 L, 1 M	25 R, 3 L	$X^2(2, n = 44) = 5.030, p = 0.81$
Full-Scale IQ, median [range]	76 [67-126]	114.5 [88−136]	$W = 808.5, p < 0.001$

Note: Full-Scale IQ was measured using the Wechsler Abbreviated Intelligence Scale (WASI) or the Wechsler Intelligence Scale for Children, 4th edition (WISC-IV; n = 3) where the mean standardised score is M = 100 and SD = 15; Handedness was estimated by the Edinburgh Handedness Inventory with the following scores: Right-handed = +40 to +100, left-handed = −40 to −100, mixed handed = −40 to +40.

whom the aberrant commissural bundles were not visualised, independent samples t-test was used.

To explore association between the observed aberrant structural bundles and functional connectivity, we used independent sample t-tests for the (a) atlas-based seeds approach and compared parietal FC in children with CD with and without the alternative bundles. For the (b) bundle-specific seeds approach, Pearson's correlations were explored between bundle-specific seed FC and number of streamlines/tract volumes/mean FA of the concerned bundles.

3 | RESULTS

3.1 | Sample characteristics

Children were included in the current study if they had completed the required MRI sequences (T1, DWI and resting-state fMRI), resulting in the exclusion of five participants from the CD group and one participant from the TDC group. After quality checking the functional and structural MR images, three CD participants were excluded from the tractography analyses, while six CD and one TDC participants were excluded from the associated functional connectivity analysis.

The characteristics of the final CD and the TDC groups used in the current study are presented in Table 1 for each of the tractography and association with FC analyses, given the samples differed for the two analyses. The tractography analyses included 20 children with CD, including 13 complete CD (four isolated, none complex, i.e., associated with other brain anomalies) and seven partial CD (three isolated, four complex)), as well as 29 TDC children aged 8 to 17 years. Analyses exploring associations between tractography and microstructural properties with FC included 16 children with CD, including 10 complete CD (three isolated, seven complex) and six partial CD (three isolated, three complex)), as well as 28 TDC children.

Of note, there was large variability in the Full-Scale IQ score for children with CD, ranging from 66 to 126, and three children had a Full-Scale IQ below 70 (i.e., two SD or more below the normative test mean, in the extremely low range). The median Full-Scale IQ score of the CD group (median = 75.5) is within the Below Average range and similar to what has been previously described in studies of individuals with CD (Siffredi et al., 2013). Moreover, there was a high proportion of left-handedness in the CD group (n = 8, 40%) and significantly more than in the TDC group (sample of the tractography analysis, p = 0.019). This is consistent with previous CD studies reporting a higher proportion of left-handedness than in the general population, ranging from 24% to 56% (e.g., (Chiarello, 1980; Labadi & Beke, 2017; Ocklenburg et al., 2015; Sauerwein & Lassonde, 1994). For further discussion of the underlying mechanisms see Genc et al., and Gunturkun (2015).

3.2 | Assessment of ventral forebrain and midbrain bundles

Illustrations of the ventral forebrain and midbrain bundles are shown on Figure 1 and Figure S1. CD children characteristics are shown in Table 2.

The ventral forebrain bundle was visualized in 6 children with CD corresponding (30% of the cohort) and in none of the TDC children, with a significant group difference in the proportion of visualization of this aberrant bundle (X2 (1, N = 49) = 9.914, p = 0.002). It was only revealed in complete CD but not in partial CD, both in complex (n = 4, 20%) and isolated CD (n = 2, 10%). Similarly, the midbrain bundle was found in six children with CD (30% of the cohort) and in two TDC (6.9% of the TDC sample), with a significant group difference in the proportion of visualization of this aberrant bundle (X2 (1, N = 49) = 4.625, p = 0.032). Of the CD children, it was observed in five children with complete CD (25%) and in one children with partial CD (5%) who had

TABLE 2 CD children characteristics

ID	Age	Sex	H	IQ	Complete or Partial CD	PB	CO	Complex CD or Isolated CD	Commissural bundles connecting parietal cortices
024*	12.67	M	R	70	C	+	+	Isolated CD	Ventral forebrain
113*	10	F	R	73	C	+	+	Isolated CD	Ventral forebrain
020*	12.67	M	L	76	C	+	–	Abnormal deep sulcation (right parietal) lined by polymicrogyria	Ventral forebrain +Midbrain
107	11.58	M	L	66	C	+	+	Left interhemispheric cyst, hypoplasia in left hemisphere.	Ventral forebrain +Midbrain
110	9	M	L	95	C	+	+	Interhemispheric cyst with saptation in left hemisphere, causing pressure in right. Cortex around cyst is malformed	Ventral forebrain +Midbrain
022*	8.67	F	M	71	C	+	–	Unusual deep sulci (right central sulcus, parasagittal region posteriorly)	Ventral forebrain +Midbrain
011	11.67	M	L	75	C	+	+	Isolated CD	Midbrain
026	14.83	F	R	74	P Rostrum, genu, anterior and thin middle anterior body remnant	–	–	Bilateral polymicrogyria	Midbrain
109*	9.67	F	R	126	P Thin rostrum, genu, anterior body remnant	+	+	Isolated CD (history of haemorrhagic cerebral AVM due to genetic condition)	No visualisation of aberrant bundles
003*	15.58	M	L	113	P Small genu remnant	+	+	Isolated CD	No visualisation of aberrant bundles
021*	10.67	M	R	84	C	+	+	Unilateral periventricular heterotopic grey matter (right frontal horn)	No visualisation of aberrant bundles
008*	11.33	M	L	67	C	+	+	Cortical dysplasia	No visualisation of aberrant bundles
012*	15.33	F	R	100	P Rostrum remnant	+	+	Bilateral periventricular heterotopic grey matter	No visualisation of aberrant bundles
015*	10.25	F	L	73	P Middle-posterior body, posterior body, splenium remnant	–	–	Abormal grey matter around frontal horns of lateral ventricles, abnormal sulci medio in frontal lobe	No visualisation of aberrant bundles
016*	16.17	F	R	100	P Anterior body remnant	+	–	Isolated CD	No visualisation of aberrant bundles
017*	8.83	F	R	71	C	+	+	Bilateral periventicular heterotopic grey matter	No visualisation of aberrant bundles
018*	14.42	M	R	67	C	+	+	Isolated CD	No visualisation of aberrant bundles
019*	11	M	R	76	C	+	+	Isolated CD	No visualisation of aberrant bundles
108	10.17	M	L	83	C	+	–	Left interhemispheric cyst, grey matter heterotopia, left anterior hemispheric cortical dysplasia	No visualisation of aberrant bundles
112*	17.08	M	R	82	P Rostrum remnant	+	+	Frontonasal dysplasia, sphenoidal encephalocele, non-visualisation of pituitary gland	No visualisation of aberrant bundles

Note: Age: in years; Sex: F female, M male; H Handedness: L left, R right, A ambidextrous; PB: probst bundles, + present,—absent; CO: colpocephaly + present,—absent; * indicate children with both diffusion and resting-state fMRI data.
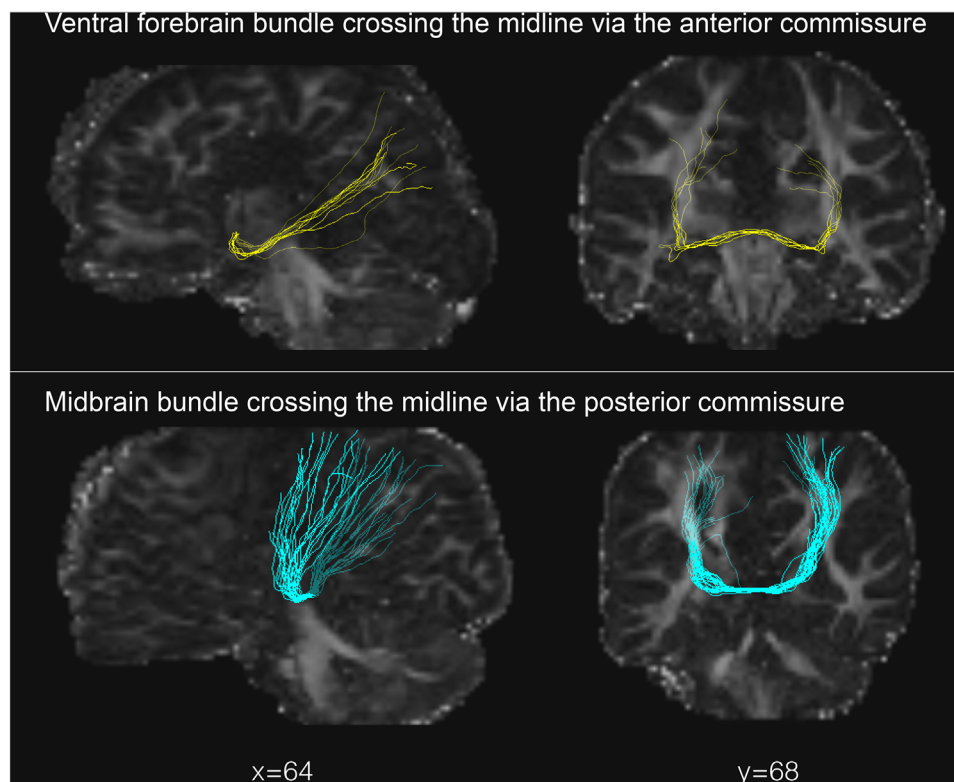
FIGURE 1   Illustration of the two aberrant homotopic bundles retrieved in children with CD, first described by Tovar-Moll et al., 2014 (participant ID: 020 for the ventral forebrain and 022 for the midbrain bundles)

remnants of the rostrum, genu, and part of the anterior body. This bundle was mostly retrieved in the context of complex CD (n = 5, 25%). The midbrain bundles observed in two TDC were comparable to those visualized in CD children. Notably, both the ventral forebrain and the midbrain bundles were visualised in four children with CD (20%).

Of note, other typical interhemispheric streamlines in the anterior and posterior commissures in our CD and the TDC groups were visualised using tractography. However, given the focus of the current study, that is, the replication of the two aberrant bundles observed by Tovar-Moll and colleagues, we only reported the fibres crossing the anterior and posterior commissures and connecting parietal areas.

3.3 | Functional connectivity associated with ventral forebrain and midbrain bundles

Based on the endpoints of the two aberrant bundles in all participants, a total of 20 homotopic regions from the Brainnetome atlas (Fan et al., 2016) in the parietal cortices (i.e., superior parietal lobule, inferior parietal lobule, and precuneus) were used as seeds, see Table S1. Using the atlas-based FC seeds approach, we did not observe robust group differences in inter-hemispheric FC of seeds in homotopic parietal regions between children with and without the ventral forebrain and/or the midbrain bundles retrieved (ranging from $p = 0.189$ to $p = 0.991$), see Table S2 and S3.

For the bundle-specific FC seeds, we used the left and the right sided endpoints of the ventral forebrain and/or midbrain bundles retrieved as FC seeds. FC was consistently low across children (ranging from $r = -0.04$ to $r = 0.29$). For both bundles, there were no robust positive correlations between the number of streamlines, tracts volumes, and mean FA with FC (ranging from $r = -0.863$ to $r = 0.713$), see Table S4.

3.4 | Group difference on general intellectual functioning (visualization of the ventral forebrain and midbrain bundles vs. no visualization)

There was no significant group difference on general intellectual functional between children with CD for whom the ventral forebrain and midbrain bundles were visualized on tractography and the ones for whom the ventral forebrain and midbrain bundles were not visualized ($t(16) = -1.295, p = 0.214; t(15) = -0.859, p = 0.404$).

4 | DISCUSSION

Brain rewiring mechanisms have been proposed in CD with the existence of alternative white-matter bundles crossing the midline through the anterior and posterior commissures and connecting parietal cortices (Tovar-Moll et al., 2014). Our findings show the presence of the ventral forebrain bundle crossing the midline via the anterior

commissures and connecting parietal cortices in 30% of children with CD. The midbrain bundle crossing the midline in the posterior commissures and connecting parietal cortices was found in 30% of the cohort. These results partially replicated those of Tovar-Moll et al. (2014).

The ventral forebrain bundle crossing though the anterior commissure was specific to CD children (and not found in TDC children) and only in cases of complete CD. This is in contrast to Tovar-Moll and colleagues, who observed the ventral forebrain bundle in an individual with partial CD (genu remnant). The midbrain bundle crossing the midline though the posterior commissure was mainly retrieved in cases of complete CD (25%), but also in partial CD (5%, remnant of the genu and part of the body). Furthermore, this bundle was not specific to children with CD as it was retrieved in TDC children (6.9%), but still showing a significant group difference in the proportion of visualization of this bundle. Notably, for 20% of our cohort of children with CD, both the ventral forebrain and the midbrain bundles were visualized. The presence of a combination of both bundles was not found in the previous study by Tovar-Moll et al. (2014). It is possible that very early disruption of embryological callosal development, and consequently a reduction of axons crossing the midline will enhance neuroplasticity and facilitates the formation of alternative neural pathways in some children with CD (Huang et al., 2009; Paul, 2011; Richards et al., 2004). Moreover, our findings suggest that these aberrant bundles are more frequently visualized in complete CD. In complete CD, the disruption of callosal development occurring slightly earlier in gestation than partial CD might lead to increase white-matter rewiring in some cases.

A major finding of this study, however, is the lack of evidence of an association between the ventral forebrain and midbrain bundles and parietal FC. Specifically, there was no difference in parietal FC between children with CD with or without at least one of the bundles. Moreover, we did not find evidence of positive association between the structural and microstructural properties of the aberrant bundles with parietal FC. These findings could also be explained by developmental processes associated with functional brain maturation occurring in a developmental sample (Supekar et al., 2009), as opposed to a sample of a large age range and including adults in the study of Tovar-Moll et al. (2014, age range: 2 to 33 years).

Additionally, we did not find evidence of association between the presence of these aberrant bundles and general intellectual functioning.

Altogether, our findings bring in to question the role and implication of these bundles in alternative pathways for interhemispheric FC.

Previous studies have shown that advanced tractography strategies in combination with current diffusion modelling techniques recover most of the valid bundles in the human brain (Maier-Hein et al., 2017). However, these studies also reveal important limitations of such strategies. For example, tractography produces thick and dense bundles of plausible looking streamlines in locations where such streamlines are not present (Maier-Hein et al., 2017; Thomas et al., 2014). Thus, false-positive bundles may be produced by tractography pipelines, questioning the validity of the presence of such aberrant bundles. Given the limitations of diffusion-weighted imaging and analysis techniques, additional studies using high quality data, for example, MRI acquisi-

tion using ultra-high field seven Tesla could help clarify the existence of these bundles in CD, as well as in the typically developing brain. If future high-quality studies were to retrieve these bundles, they should additionally examine their potential role in motor and neurodevelopmental outcomes in CD.

DATA AVAILABILITY STATEMENT

Ethical restrictions prevent us from making anonymized data available in a public repository. Appropriate ethical approval is required prior to release and only de-identified data will be available (contact Vicki.Anderson@rch.org.au).

CONFLICT OF INTEREST

There is no conflict of interests to report.

REFERENCES

Bénézit, A., Hertz-Pannier, L., Dehaene-Lambertz, G., Monzalvo, K., Germanaud, D., Duclap, D., Guevara, P., Mangin, J.-F., Poupon, C., Moutard, M.-L., & Dubois, J. (2015). Organising white matter in a brain without corpus callosum fibres. *Cortex*, *63*, 155–171.

Bolton, T. A., Morgenroth, E., Preti, M. G., & Van De Ville, D. (2020). Tapping into multi-faceted human behavior and psychopathology using fMRI brain dynamics. *Trends in Neurosciences*, *43*(9), 667–680.

Catani, M., & Thiebaut de Schotten, M. (2008). A diffusion tensor imaging tractography atlas for virtual in vivo dissections. *Cortex*, *44*(8), 1105–1132. https://doi.org/10.1016/j.cortex.2008.05.004

Chiarello, C. (1980). A house divided? Cognitive functioning with callosal agenesis. *Brain and Language*, *11*(1), 128–158. https://doi.org/10.1016/0093-934x(80)90116-9

Dennis, M. (1976). Impaired sensory and motor differentiation with corpus callosum agenesis: a lack of callosal inhibition during ontogeny? *Neuropsychologia*, *14*(4), 455–469. https://doi.org/10.1016/0028-3932(76)90074-9

Edwards, T. J., Sherr, E. H., Barkovich, A. J., & Richards, L. J. (2014). Clinical, genetic and imaging findings identify new causes for corpus callosum development syndromes. *Brain*, *137*, 1579–1613. https://doi.org/10.1093/brain/awt358

Fan, L., Li, H., Zhuo, J., Zhang, Y., Wang, J., Chen, L., Yang, Z., Chu, C., Xie, S., Laird, A. R., Fox, P. T., Eickhoff, S. B., Yu, C., & Jiang, T. (2016). The Human Brainnetome Atlas: a New Brain Atlas Based on Connectional

Architecture. *Cerebral Cortex*, *26*(8), 3508–3526. https://doi.org/10.1093/cercor/bhw157

Gazzaniga, M. S. (2000). Cerebral specialization and interhemispheric communication: does the corpus callosum enable the human condition? *Brain*, *123*(Pt 7), 1293–1326.

Genc, E., Ocklenburg, S., Singer, W., & Gunturkun, O. (2015). Abnormal interhemispheric motor interactions in patients with callosal agenesis. *Behavioural Brain Research*, *293*, 1–9. https://doi.org/10.1016/j.bbr.2015.07.016

Giedd, J. N., Rumsey, J. M., Castallanos, F. X., Rajapakse, J. C., Kaysen, D., Vaituzis, A. C., Vauss, Y. C., Hamburger, S. D., & Rapoport, J. L. (1996). A quantitative MRI study of the corpus callosum in children and adolescents. *Brain Research: Developmental Brain Research*, *91*, 274–280.

Huang, H., Xue, R., Zhang, J., Ren, T., Richards, L. J., Yarowsky, P., Miller, M. I., & Mori, S. (2009). Anatomical characterization of human fetal brain development with diffusion tensor magnetic resonance imaging. *The Journal of Neuroscience*, *29*(13), 4263–4273.

Keene, M. F. (1938). The connexions of the posterior commissure: a study of its development and myelination in the human foetus and young infant, of its phylogenetic development, and of degenerative changes resulting from certain experimental lesions. *Journal of Anatomy*, *72*, 488–501.

Kollias, S. (2012). Insights into the connectivity of the human brain using DTI. *Nepalese Journal of Radiology*, *1*(1), 78–91.

Labadi, B., & Beke, A. M. (2017). Mental state understanding in children with agenesis of the corpus callosum. *Frontiers in Psychology*, *8*, 94. https://doi.org/10.3389/fpsyg.2017.00094

Leonardi, N., Richiardi, J., Gschwind, M., Simioni, S., Annoni, J. M., Schluep, M., Vuilleumier, P., & Van De Ville, D. (2013). Principal components of functional connectivity: a new approach to study dynamic brain connectivity during rest. *NeuroImage*, *83*, 937–950. https://doi.org/10.1016/j.neuroimage.2013.07.019

Maier-Hein, K. H., Neher, P. F., Houde, J. C., Côté, M. A., Garyfallidis, E., Zhong, J., Chamberland, M., Yeh, F. C., Lin, Y. C., Ji, Q., Reddick, W. E., Glass, J. O., Chen, D. Q., Feng, Y., Gao, C., Wu, Y., Ma, J., He, R., Li, Q., & … Descoteaux, M. (2017). The challenge of mapping the human connectome based on diffusion tractography. *Nature Communication*, *8*(1), 1–13.

Mancuso, L., Uddin, L. Q., Nani, A., Costa, T., & Cauda, F. (2019). Brain functional connectivity in individuals with callosotomy and agenesis of the corpus callosum: a systematic review. *Neuroscience Biobehavioral Reviews*, *105*, 231–248.

Meoded, A., Katipally, R., Bosemani, T., Huisman, T. A., & Poretti, A. (2015). Structural connectivity analysis reveals abnormal brain connections in agenesis of the corpus callosum in children. *European Radiology*, *25*(5), 1471–1478. https://doi.org/10.1007/s00330-014-3541-y

Obertino, S., Hernández, S. J., Galazzo, I. B., Pizzini, F. B., Zucchelli, M., & Menegaz, G. (2017). Exploiting Machine Learning Principles for Assessing the Fingerprinting Potential of Connectivity Features. Paper presented at the Computational Diffusion MRI Workshop (CDMRI) of International Conference on Medical Image Computing and Computer-Assisted Intervention (MICCAI).

Ocklenburg, S., Ball, A., Wolf, C. C., Genc, E., & Gunturkun, O. (2015). Functional cerebral lateralization and interhemispheric interaction in patients with callosal agenesis. *Neuropsychology*, *29*(5), 806–815. https://doi.org/10.1037/neu0000193

Owen, J. P., Li, Y. O., Ziv, E., Strominger, Z., Gold, J., Bukhpun, P., Wakahiro, M., Friedman, E. J., Sherr, E. H., & Mukherjee, P. (2013). The structural connectome of the human brain in agenesis of the corpus callosum. *NeuroImage*, *70*, 340–355. https://doi.org/10.1016/j.neuroimage.2012.12.031

Paul, L. K. (2011). Developmental malformation of the corpus callosum: a review of typical callosal development and examples of developmental disorders with callosal involvement. *Journal of Neurodevelopmental Disorders*, *3*(1), 3–27. https://doi.org/10.1007/s11689-010-9059-y

Paul, L. K., Brown, W. S., Adolphs, R., Tyszka, J. M., Richards, L. J., Mukherjee, P., & Sherr, E. H. (2007). Agenesis of the corpus callosum: genetic, devel-

opmental and functional aspects of connectivity. *Nature Reviews Neuroscience*, *8*(4), 287–299.

Power, J. D., Barnes, K. A., Snyder, A. Z., Schlaggar, B. L., & Petersen, S. E. (2012). Spurious but systematic correlations in functional connectivity MRI networks arise from subject motion. *Neuroimage*, *59*(3), 2142–2154. https://doi.org/10.1016/j.neuroimage.2011.10.018

Power, J. D., Mitra, A., Laumann, T. O., Snyder, A. Z., Schlaggar, B. L., & Petersen, S. E. (2014). Methods to detect, characterize, and remove motion artifact in resting state fMRI. *NeuroImage*, *84*, 320–341. https://doi.org/10.1016/j.neuroimage.2013.08.048

Preti, M. G., & Van De Ville, D. (2017). Dynamics of functional connectivity at high spatial resolution reveal long-range interactions and fine-scale organization. *Scientific Reports*, *7*(1), 1–12. https://doi.org/10.1038/s41598-017-12993-1

Pujol, J., Vendrell, P., Junque, C., Marti-Vilalta, J. L., & Capdevila, A. (1993). When does human brain development end? Evidence of corpus callosum growth up to adulthood. *Annals of Neurology*, *34*, 71–75.

Richards, L. J., Planchez, C., & Ren, T. (2004). Mechanisms regulating the development of the corpus callosum and its agenesis in mouse and human. *Clinical Genetics*, *66*, 276–289.

Sauerwein, H. C., & Lassonde, M. (1994). Cognitive and sensori-motor functioning in the absence of the corpus callosum: neuropsychological studies in callosal agenesis and callosotomized patients. *Behavioural Brain Research*, *64*(1-2), 229–240.

Siffredi, V., Anderson, V., Leventer, R. J., & Spencer-Smith, M. M. (2013). Neuropsychological profile of agenesis of the corpus callosum: a systematic review. *Developmental Neuropsychology*, *38*(1), 36–57. https://doi.org/10.1080/87565641.2012.721421

Siffredi, V., Anderson, V., McIlroy, A., Wood, A. G., Leventer, R. J., & Spencer-Smith, M. M. (2018). A neuropsychological profile for agenesis of the corpus callosum? Cognitive, academic, executive, social, and behavioral functioning in school-age children. *Journal of International Neuropsychology Society*, *24*(5), 445–455. https://doi.org/10.1017/S1355617717001357

Siffredi, V., Preti, M. G., Kebets, V., Obertino, S., Leventer, R. J., McIlroy, A., Wood, A. G., Anderson, V., Spencer-Smith, M. M., & Van De Ville, D. (2020). Structural neuroplastic responses preserve functional connectivity and neurobehavioural outcomes in children born without corpus callosum. *Cerebral Cortex*, *31*(2), 1227–1239. https://doi.org/10.1093/cercor/bhaa289

Siffredi, V., Wood, A. G., Leventer, R. J., Vaessen, M., McIlroy, A., Anderson, V., Vuilleumier, P., & Spencer-Smith, M. M. (2019). Anterior and posterior commissures in agenesis of the corpus callosum: alternative pathways for attention processes? *Cortex*, *121*, 454–467.

Smith, R. E., Tournier, J. D., Calamante, F., & Connelly, A. (2013). SIFT: spherical-deconvolution informed filtering of tractograms. *NeuroImage*, *67*, 298–312. https://doi.org/10.1016/j.neuroimage.2012.11.049

Smith, S. M. (2002). Fast robust automated brain extraction. *Human Brain Mapping*, *17*(3), 143–155. https://doi.org/10.1002/hbm.10062

Supekar, K., Musen, M., & Menon, V. (2009). Development of large-scale functional brain networks in children. *PLoS Biol*, *7*(7), e1000157.

Tax, C. M., Jeurissen, B., Vos, S. B., Viergever, M. A., & Leemans, A. (2014). Recursive calibration of the fiber response function for spherical deconvolution of diffusion MRI data. *NeuroImage*, *86*, 67–80. https://doi.org/10.1016/j.neuroimage.2013.07.067

Thomas, C., Frank, Q. Y., Irfanoglu, M. O., Modi, P., Saleem, K. S., Leopold, D. A., & Pierpaoli, C. (2014). Anatomical accuracy of brain connections derived from diffusion MRI tractography is inherently limited. *Proceedings of the National Academy of Sciences*, *111*(46), 16574–16579.

Tournier, J. D., Calamante, F., & Connelly, A. (2012). MRtrix: diffusion tractography in crossing fiber regions. *International journal of imaging systems and technology*, *22*(1), 53–66.

Tournier, J. D., Calamante, F., & Connelly, A. (2007). Robust determination of the fibre orientation distribution in diffusion MRI: non-negativity

constrained super-resolved spherical deconvolution. *NeuroImage*, *35*(4), 1459–1472. https://doi.org/10.1016/j.neuroimage.2007.02.016

Tournier, J. D., Yeh, C. H., Calamante, F., Cho, K. H., Connelly, A., & Lin, C. P. (2008). Resolving crossing fibres using constrained spherical deconvolution: validation using diffusion-weighted imaging phantom data. *Neuroimage*, *42*(2), 617–625. https://doi.org/10.1016/j.neuroimage.2008.05.002

Tovar-Moll, F., Monteiro, M., Andrade, J., Bramati, I. E., Vianna-Barbosa, R., Marins, T., Marins, T., Rodrigues, E., Dantas, N., Behrens, T. E., de Oliveira-Souza, R., Moll, J., & Lent, R. (2014). Structural and functional brain rewiring clarifies preserved interhemispheric transfer in humans born without the corpus callosum. *Proceedings of the National Academy of Sciences of the United States of America: PNAS*, *111*(21), 7843–7848. https://doi.org/10.1073/pnas.1400806111

Tyszka, J. M., Kennedy, D. P., Adolphs, R., & Paul, L. K. (2011). Intact bilateral resting-state networks in the absence of the corpus callosum. *Journal of Neuroscience*, *31*(42), 15154–15162.

Uddin, L. Q., Supekar, K., & Menon, V. (2010). Typical and atypical development of functional human brain networks: insights from resting-state FMRI. *Frontiers in Systems Neuroscience*, *4*, 21.

Wechsler, D. (1999). *Wechsler Abbreviated Scale of Intelligence (WASI)*. San Antonio, TX: Psychological Corporation.

Wechsler, D. (2003). *Manual for the Wechsler Intelligence Scale for Children-IV*. New York: Psychological Corporation.

Yuan, J., Song, X., Kuan, E., Wang, S., Zuo, L., Ongur, D., Hu, W., & Du, F. (2020). The structural basis for interhemispheric functional connectivity: evidence from individuals with agenesis of the corpus callosum. *NeuroImage: Clinical*, *28*, 102425.

SUPPORTING INFORMATION

Additional supporting information may be found online in the Supporting Information section at the end of the article.